International Journal of Thermophysics, Vol. 11, No. 4, 1990

Measurement of Thermophysical Properties of Lead by a Submicrosecond Pulse-Heating Method in the Range 2000–5000 K[1]

G. Pottlacher[2] and H. Jäger[2]

A submicrosecond ohmic pulse-heating technique with heating rates of more than $10^9\ K \cdot s^{-1}$ allows the determination of such thermophysical properties as heat capacity and the mutual dependences among enthalpy, electrical resistivity, temperature, and volume up to superheated liquid states for lead. Also, an estimation of the critical point data is given from investigations at elevated static pressures.

KEY WORDS: critical data; dynamic measurements; electrical resistivity; enthalpy; high pressures; high temperatures; lead; liquid metal; specific heat.

1. INTRODUCTION

About 80% of the elements are metals. Their thermophysical and electrical behavior is reasonably well known in the solid state. The liquid state of metals is more difficult to investigate. It covers the temperature range from the melting point up to the critical temperature, which, for some metals, is more than 10,000 K. Dynamic measurements have been developed for the investigation of thermophysical properties at these temperatures. A general survey of pulse techniques with resistive heating of the specimen is given by Cezairliyan [1].

For the investigation of critical point data of metals, additionally high pressures have to be applied if one excludes the alkali metals and mercury (for a summary of alkali critical-point data see Ohse et al. [2]; for mercury

[1] Paper presented at the First Workshop on Subsecond Thermophysics, June 20–21, 1988, Gaithersburg, Maryland, U.S.A.

[2] Institut für Experimentalphysik, Technische Universität Graz, Petersgasse 16, 8010 Graz, Austria.

0195-928X/90/0700-0719$06.00/0

see Hensel et al. [3]). Gathers [4] reviews dynamic high-temperature and high-pressure techniques and gives a summary of theoretical and experimentally obtained critical data of metals.

Gathers' summary shows that a lot of theoretical estimations of critical data for metals exist, but because of the great experimental difficulties in these temperature regions at elevated pressures only a few experimental investigations have been performed.

From estimations based on experiments of Hixson et al. [5] and of Hodgson [6] about the location of the critical point of Pb, we were encouraged to study fluid Pb in the critical region, as our capacitor discharge circuit can achieve heating rates of $10^9\ \mathrm{K \cdot s^{-1}}$ and the containment vessel used has a maximum pressure capability of 0.5 GPa.

2. EXPERIMENTAL

The experiments reported here were performed with a coaxially built fast (submicrosecond) RCL discharge circuit (energy storage capacitive; short circuit ringing period, 6.2 μs; $R = 26.3\ \mathrm{m\Omega}$; $C = 5.4\ \mu\mathrm{F}$; $L = 180\ \mathrm{nH}$). The details of the experimental setup and of the measuring technique are reported in earlier publications [7, 8].

The lead wires used in this work had typically dimensions of 40 mm in length and 0.25 mm or 0.5 mm in diameter. Goodfellow (Cambridge, UK) reports for the purity 99.99 + %. The wire sample is resistively heated. Water was used as the surrounding medium to avoid peripheral gas discharges. We investigated under variation of the water pressure from 0.1 MPa up to 0.5 GPa.

Figure 1 shows the way we determined the different thermophysical properties. Time-dependent quantities at different static pressures of the surrounding medium were measured during the heating process: the current $I(t)$ with an induction coil and subsequent RC integration, the voltage drop $U(t)$ across the wire with a coaxially ohmic voltage divider, the surface radiance temperature $J(t)$ of the wire with the photodiode of a fast pyrometer (operating at 800 nm), and the expansion of the wire at any desired point of the investigated time interval with the help of a Kerrcell camera (exposure time, 30 ns) which gives the wire radius $r(t)$ and thus the volume expansion V/V_0.

By subtraction of the inductive voltage components one obtains the "corrected" voltage $U_c(t)$. This voltage and the current allow the determination of the time-dependent enthalpy $H(t)$ and the electrical resistivity $\rho_0(t)$. The index zero means that in calculating this value, thermal expansion did not need to be taken into account. Using this value, it was found

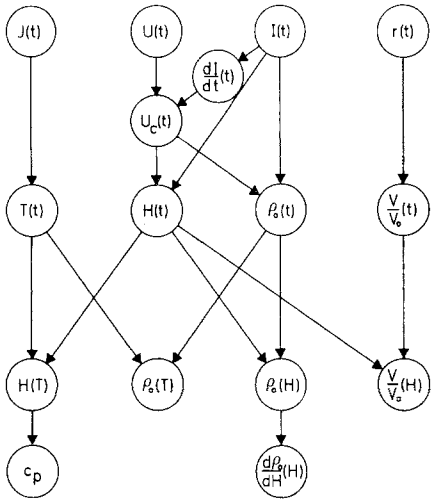

Fig. 1. Measured and determined quantities. J, surface radiance; U, voltage; I, current; r, wire radius; t, time; T, temperature; H, enthalpy; ρ_0, electrical resistivity without volume correction; V/V_0, volume expansion; c_p, specific heat.

that the wire expansion at the end of the pure liquid phase appears more characteristic in the corresponding graphs (see, e.g., Figs. 3 and 4).

Calculation of the temperature $T(t)$ from the radiation intensity could not be done without some restricting assumptions. Our pyrometer is not sensitive for temperatures below 2000 K. To perform temperature measurements at least one calibration point is needed. If the surface radiance of the melting metal can be detected by the pyrometer, the known melting temperature of the specimen can serve as a calibration point. Temperature calculations [8] according to Kirchhoff–Planck law are then usually made under the assumption that the emissivity at the melting point stays constant throughout the liquid phase. This means that using this method, we will be able to investigate metals with melting temperatures higher than 2000 K.

With the help of the melting transition of tantalum as the calibration point, we were able to measure temperature dependences of enthalpy and resistivity of nickel and iron (melting transition below 2000 K), which showed a good agreement with values given in the literature [9]. This method requires two emissivity values: one from the melting point of the metal which serves as the radiation reference and one from the melting point of the metal to be investigated. Again, the assumption is made that

the emissivity of the investigated metal remains constant during the liquid phase. For the temperature measurements on liquid lead, tantalum was used again as the calibration point.

Eliminating the time dependence of the values from the second row in Fig. 1, one arrives at the third row with the interdependence of enthalpy, resistivity, temperature, and volume expansion. Measuring these quantities under varying static pressure on the wire sample, estimations of the critical point data of lead should be possible.

3. PREVIOUS CONSIDERATIONS

Figure 2 shows a schematic phase diagram in the $p - V$ plane. Three main areas are the region of solid state (s), of liquid state (1), and of gaseous state (g). Mixtures where two states at the same time can exist are the solid–liquid region (between the s and the l region), the liquid–vapor region (l + v), and the solid–vapor region (s + v). The line A–K is known as the normal boiling line, A–K–D is the binodal. The line B–K–C represents the spinodal line; K is the critical point.

The binodal line is the equilibrium curve for liquid and vapor; in the region A–K–B a mixture of liquid and vapor as well as a superheated

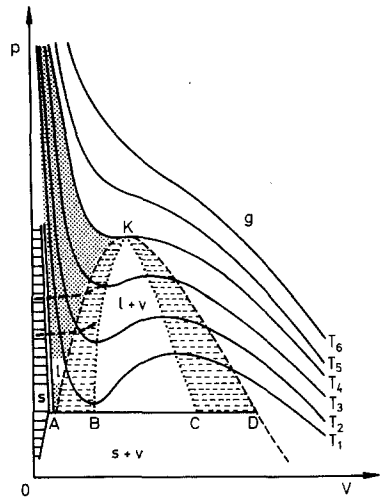

Fig. 2. Schematic Van der Waals phase diagram in the $p - V$ plane. Isotherms $T_1 < T_2 < T_3 < T_4 < T_5 < T_6$; T_4, critical isotherm; A–K–D, binodal line; B–K–C, spinodal line; *K*, critical point; s, solid; l, liquid; v, vapor; g, gas. Broken line, path of our experiment.

liquid state can exist. The spinodal line B–K is the boundary of thermodynamic stability of the superheated metastabile liquid. Using high heating rates we can superheat liquid metals up to the spinodal line [10]. Near the spinodal volume fluctuations begin (sudden growth of homogeneous vapor nuclei in the superheated liquid; see, e.g., Refs. 4 and 11). The area within B–K–C is unstable and therefore a "jump" into the region K–C–D (the so-called phase explosion [11]) with a large increase in volume will occur. At this moment the resistivity of the sample starts to increase steeply.

Possible changes of the state variables during our pulse heating experiment, at two different static pressures, are drawn as broken lines in Fig. 2. The sample is heated from the solid state to the melting transition and through the liquid region into the region of metastabile superheated liquid. The normal boiling point of lead is about 2000 K. We reach temperatures up to 5000 K. In that metastabile region, a slight increase in pressure will occur because of the volume expansion and the interaction with the surrounding water. Calculations of Fucke and Seydel [12] show that, at elevated pressures of 0.4 GPa, these dynamic components do not exceed 0.02 GPa for an experiment similar to ours.

Crossing the spinodal line causes a sharp increase in the electrical resistivity, as the conducting cross section of the sample is reduced. The rapid creation of vapor nuclei connected with a powerful expansion, the so-called phase explosion, produces a shock wave in the surrounding medium. At that moment the surface temperature starts to decrease due to the cooling of the liquid phase as it looses the more energetic atoms to the vapor phase, which expands adiabatically [12].

For the experimental determination of critical point data, we proceeded the way Seydel and Fucke [11] suggested for fast pulse experiments: if the static pressure p_s is increased, the sharp rise in the electrical resistivity will occur at higher enthalpy values and the shock wave would become weaker. At static pressures higher than the critical pressure the shock wave and the sharp rise of the electrical resistivity should vanish. This might be a direct method to determine p_c. When reaching the spinodal line, the critical temperature T_c can be calculated from the corresponding enthalpy values. The volume expansion versus enthalpy curve gives the critical volume v_c.

4. RESULTS

As can be seen from Fig. 1, time-resolved measurements of voltage and current allow the determination of the time dependence of enthalpy and electrical resistivity as well as the electrical resistivity as a function of

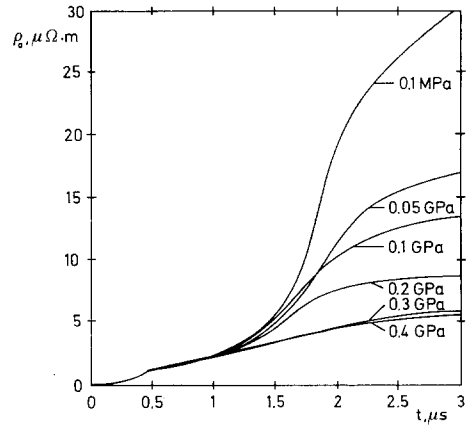

Fig. 3. Electrical resistivity without volume correction ρ_0 as a function of time t at different static pressures.

enthalpy. The pressure dependence of the electrical resistivity versus time for this experiment is given in Fig. 3.

The melting transition is reached after about 0.5 μs; during the liquid phase up to about 1 μs no essential pressure dependence can be observed. The steep rise of electrical resistivity starts for 0.1 MPa at about 1.5 μs. With increasing pressure the resistivity rise becomes weaker and is shifted back on the time scale. For static pressures of 0.3 and 0.4 GPa no steep electrical resistivity rise occurs.

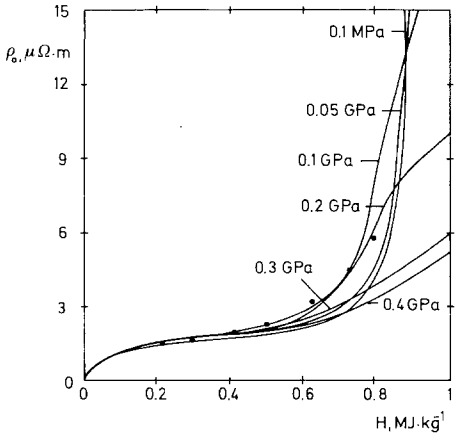

Fig. 4. Electrical resistivity without volume correction ρ_0 versus enthalpy H at different static pressures. Data points from Hodgson [6] for 0.1 GPa.

Figure 4 gives the dependence of electrical resistivity on enthalpy at different static pressures. The data points are that from Hodgson [6] for 0.1 GPa and match our curves for 0.2 GPa fairly well. The behavior for 0.1 MPa and 0.05 GPa is quite similar; at enthalpy values of about 0.85 $MJ \cdot kg^{-1}$ a strong increase in the electrical resistivity can be found. For 0.1 and 0.2 GPa a strong increase can still be detected. The values measured at 0.3 and 0.4 GPa do not show this resistivity increase.

The change of the slopes in Fig. 4 can be better demonstrated by drawing the derivative $(d\rho/dH)$ as a function of enthalpy, shown in Fig. 5. As can be seen the strongest change occurs for enthalpy values of about 0.8 $MJ \cdot kg^{-1}$, at higher static pressures the peak gets weaker, and above 0.25 GPa no changes occur.

In comparison with other metals investigated so far, the facts that the emissivity of liquid lead is not known and that our pyrometer was not sensitive below 2000 K strongly increase the uncertainty of these temperature dependences.

Figure 6 presents the enthalpy as a function of temperature. For curve 1, we took the emissivity values for lead, $\varepsilon_{Pb} = 0.18$, from Hodgson [6] and for tantalum, $\varepsilon_{Ta} = 0.34$, from Cezairliyan et al. [13]. Hodgson's [6] $H(T)$ data are given in curve 2. They lie lower than our values but within our experimental uncertainty. Curve 3 was evaluated under the arbitrary assumption of the ratio $\varepsilon_{Pb}/\varepsilon_{Ta}$ to be 0.8 (emissivities at melting point), in order to see the influence of the emissivity data on the calculated temperature values. It was found that up to static pressures of 0.4 GPa, a pressure dependence is within our experimental uncertainty.

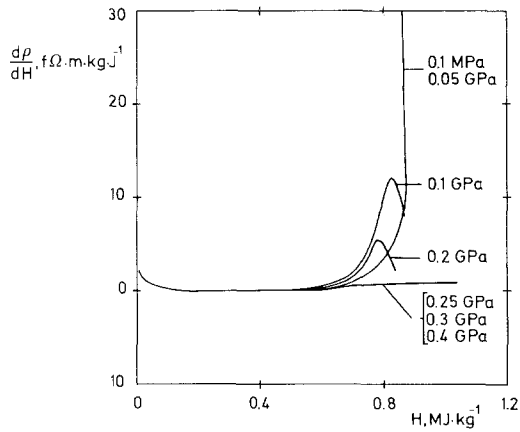

Fig. 5. Change of slope $(d\rho_0/dH)$ from Fig. 4 versus enthalpy H at different static pressures.

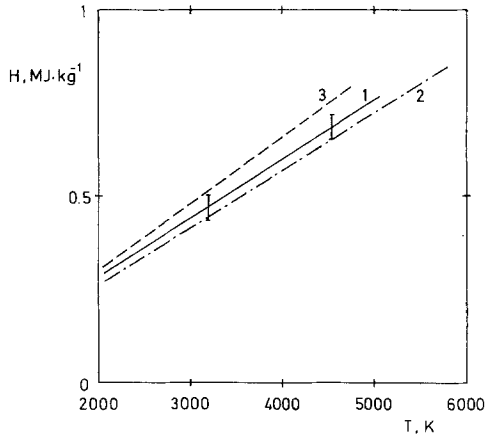

Fig. 6. Enthalpy H versus temperature T. 1, ratio $\varepsilon_{Pb}/\varepsilon_{Ta} = 0.53$; 2, Hodgson [6]; 3, ratio $\varepsilon_{Pb}/\varepsilon_{Ta} = 0.8$.

A least-squares fit in the range $2000 < T < 5000$ K can be represented by

$$H = -0.024 + 0.156 \times 10^{-3}\, T \tag{1}$$

where H is in $\mathrm{MJ \cdot kg^{-1}}$. The derivative of this polynomial gives $c_p = 156\ \mathrm{J \cdot kg^{-1} \cdot K^{-1}}$ for the specific heat of liquid lead. Hodgson's [6] value for c_p, used by Hixson et al. [5], is $157\ \mathrm{J \cdot kg^{-1} \cdot K^{-1}}$ and is, in spite of all these uncertainties, in good agreement for the slopes of curve 1 and 2.

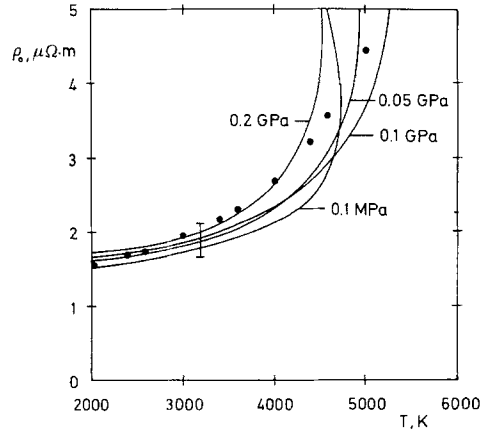

Fig. 7. Electrical resistivity without volume correction ρ_0 versus temperature T at different static pressures. Data points from Hodgson [6] for 0.1 GPa.

For some experiments, the electric resistivity as a function of temperature for different static pressures is given in Fig. 7. The data points represent the values of Hodgson [6] for 0.1 GPa. Although a large error bar should be considered in this figure, a rise in the electrical resistivity at the highest temperatures can be seen. During all these experiments we could not reach temperatures of more than 5400 K.

To handle thin wires (40-mm length, 0.25-mm diameter) of lead is not easy. Nonuniformities in the diameter will cause instability at this point when pulse heated. Therefore it was necessary to monitor the sample geometry during rapid heating. For this purpose, snapshots of the expanding wire with the help of a Kerrcell camera were taken.

At a static pressure of 0.1 MPa the sample showed a uniform geometry up to 1 μs. But it was not always possible to keep the diameter of the wire constant over its entire length. Higher local heating rates occurred at places with smaller diameters. On such points the spinodal line is reached earlier, thus leading to a local phase explosion, which becomes the center of a spherical shock wave. Increasing the static pressure kept the lead sample stable up to more than 3 μs along the full sample length. Above 0.25 MPa those spherical shock waves vanished, although the shock wave from the melting transition was still visible. Electrical measurements were evaluated only if it could be assumed that such instabilities did not occur during the interval of interest.

The relative volume change versus enthalpy for lead at two different static pressures is given in Fig. 8. At a static pressure of 0.1 MPa, a strong increase in volume expansion at enthalpy values of about 0.85 MJ $\cdot$ kg^{-1} is

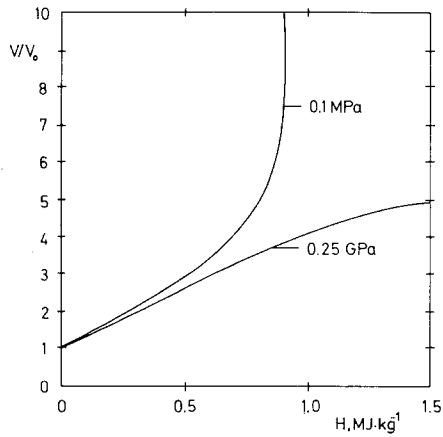

Fig. 8. Volume expansion V/V_0 versus enthalpy H at different static pressures.

found. Such strong volume increases cannot be detected for a static pressure of 0.25 GPa. This behavior of sample geometry is in agreement with that of electrical resistivity in Fig. 3 for these two pressures.

The slow increase in resistivity above static pressures of about 0.25 GPa can be seen in Figs. 3 and 4. This and the fact that Kerrcell photographs for this pressure do not show shock waves from local phase explosions indicate a critical pressure of about 0.25 GPa for lead. The strong increase in resistivity occurs for enthalpy values greater than $0.85\ \mathrm{MJ \cdot kg^{-1}}$. Under these conditions, apparently the spinodal line is reached. The uncertainty of measurements of the electrical quantities for these experiments is much smaller than that of temperature measurements. From Fig. 4, a critical temperature can be estimated: with a "critical enthalpy" of about $0.85\ \mathrm{MJ \cdot kg^{-1}}$ and Eq. (1) for liquid lead, a critical temperature of about 5400 K is calculated. Figure 7 shows that temperatures above 5400 K cannot be reached in the present experiments. This would indicate a critical temperature in the range of 5000–5500 K. From Fig. 8 we obtain a value of about 3.6 for V/V_0 corresponding to enthalpy values of about $0.85\ \mathrm{MJ \cdot kg^{-1}}$.

In Table I, a summary of experimentally determined and theoretically estimated critical point data for lead is given.

Table I. Summary of Experimentally Determined (*) or Theoretically Estimated (#) Critical-Point Data of Lead

Reference	T_k (K)	p_k (GPa)	V_k ($\mathrm{cm^3 \cdot mol^{-1}}$)	V_k/V_0	
This work	5400 ± 400	0.250 ± 0.030	65 ± 5	3.6 ± 0.4	*
Gates and Thodos [14]	3584	0.042	206	11.3	#
Carlson et al. [15]	6266	0.253	68	3.7	#
Zadumkin [16]	4200				#
Grosse and Kirshenbaum [17]	5400	0.085	96	5.1	#
Morris [18]	5400	0.140	101	5.5	#
Kopp [19]	4760				#
Bohdansky [20]	5500				#
Young and Alder [21]	4668	0.208	67	3.6	#
Fortov et al. [22], Kolgatin and Khachatur'yants [28]	4980	0.184	62	3.4	#
Martinyuk and Karimkhodzhaev [23]	3970	0.016			*
Hornung [24]	5500	0.101	82	4.5	#
Young [25]	5158	0.226	67	3.7	#
Fortov [26]	5300	0.170	89	4.9	#
Lang [27]	5150				#
Hodgson [6]	5300–6000	0.200–0.300	65	3.6–3.7	*

5. ESTIMATE OF ERRORS

A detailed analysis of errors for these measurements has been reported earlier [7, 8] and gives an uncertainty of 5% for the enthalpy and the electrical resistivity. The uncertainty of these quantities increases to about 10% when the spinodal line is reached. The indirect temperature measurements are estimated to be uncertain by as much as 25%. The static pressure in the surrounding water can be measured to within 2%. The estimated errors of the obtained critical point data are given in Table I.

REFERENCES

1. A. Cezairliyan, in *Compendium of Thermophysical Property Measurements Methods, Vol. 1*, K. D. Maglić, A. Cezairliyan, and V. E. Peletsky, eds. (Plenum Press, New York, 1984), Chap. 16, p. 643.
2. R. W. Ohse, J. F. Babelot, J. F. Magill, and M. Tetenbaum, in *Handbook of Thermodynamic and Transport Properties of Alkali-Metals*, R. W. Ohse, ed. (Blackwell Scientific, 1985), Chap. 6.1, p. 329.
3. F. Hensel, M. Yao, and H. Uchtmann, *Phil. Mag. B* **52**:499 (1985).
4. G. R. Gathers, *Rep. Prog. Phys.* **49**:341 (1986).
5. R. S. Hixson, M. A. Winkler, and J. W. Shaner, *Physica* **139/140B**:893 (1986).
6. W. M. Hodgson, Ph.D. thesis, UCRL-52498 (1978).
7. R. Gallob, H. Jäger, and G. Pottlacher, *High Temp. High Press.* **17**:207 (1985).
8. R. Gallob, H. Jäger, and G. Pottlacher, *Int. J. Thermophys.* **7**:139 (1986).
9. G. Pottlacher, H. Jäger, and T. Neger, *High Temp. High Press.* **19**:19 (1987).
10. R. Gallob, Ph.D. thesis (Technical University, Graz, 1982).
11. U. Seydel and W. Fucke, *J. Phys. F Metal. Phys.* **8**:L157 (1978).
12. W. Fucke and U. Seydel, *High Temp. High Press.* **12**:419 (1980).
13. A. Cezairliyan, J. L. McClure, L. Coslovi, F. Righini, and A. Rosso, *High Temp. High Press.* **8**:103 (1976).
14. D. S. Gates and G. Thodos, *Am. Inst. Chem. Eng. J.* **6**:50 (1960).
15. C. M. Carlson, H. Eyring, and T. Ree, *Proc. Natl. Acad. Sci. USA* **46**:649 (1960).
16. S. I. Zadumkin, *Inzh. Fiz. Zh.* **3**:63 (1960).
17. A. V. Grosse and A. D. Kirshenbaum, *J. Inorg. Nucl. Chem.* **22**:739 (1962).
18. E. Morris, AWRE Report No. 0-67/64 (London, UKAEA, 1964).
19. I. Z. Kopp, *Russ. J. Phys. Chem.* **41**:782 (1967).
20. J. Bohdansky, *L. Chem. Phys.* **49**:2982 (1968).
21. D. A. Young and B. J. Alder, *Phys. Rev. A* **3**:364 (1971).
22. V. E. Fortov, A. N. Dremin, and A. A. Leont'ev, *Teplofiz. Vysokikh Temp.* **13**:1072 (1974).
23. M. M. Martynyuk and I. Karimkhodzhaev, *Sov. Phys. Tech. Phys.* **19**:1454 (1975).
24. K. Hornung, *J. Appl. Phys.* **46**:2548 (1975).
25. D. A. Young, UCRL-52352 (Lawrence Livermore National Laboratory, 1977).
26. V. E. Fortov, Personal communication via Shaner (1977) (from Refs. 6 and 25).
27. G. Lang, *Z. Metallkunde* **68**:213 (1977).
28. S. N. Kolgatin and A. V. Khachatur'yants, *High Temp.* **20**:380 (1982).